TECHNICAL OVERVIEW · LEVEL 8+

Neutrinovoltaic®

Master Edition

The Physics, the Master Formula, and the Multilayer Architecture

Neutrino Energy Group

neutrino-energy.com

2026

Why This Matters

A server rack draws power every second it runs, and it does not care whether the sun is up. Neither does a hospital ventilator, a cold-chain refrigerator, or a remote sensor network. Batteries store energy, but they deplete. Solar panels generate electricity, but only when the sun is above the horizon. Wind turbines generate electricity, but only when air moves fast enough to turn a blade. None of these systems is continuous. The energy challenge of the next decade is generating power continuously, at the point of use, without depending on fuel logistics, weather, or a grid connection.

The ambient environment already carries continuous energetic flux: neutrinos, cosmic muons, electromagnetic background fields, thermal gradients, mechanical vibration. All of it is present everywhere on Earth, at every hour, without interruption. For most of the history of physics these fluxes were treated as noise, too weak and too diffuse to use. What follows is the physical framework, the material architecture, and the conversion chain the Neutrino Energy Group has built in response to that opportunity, and the historical record that establishes it did not have to invent the physics to do so.

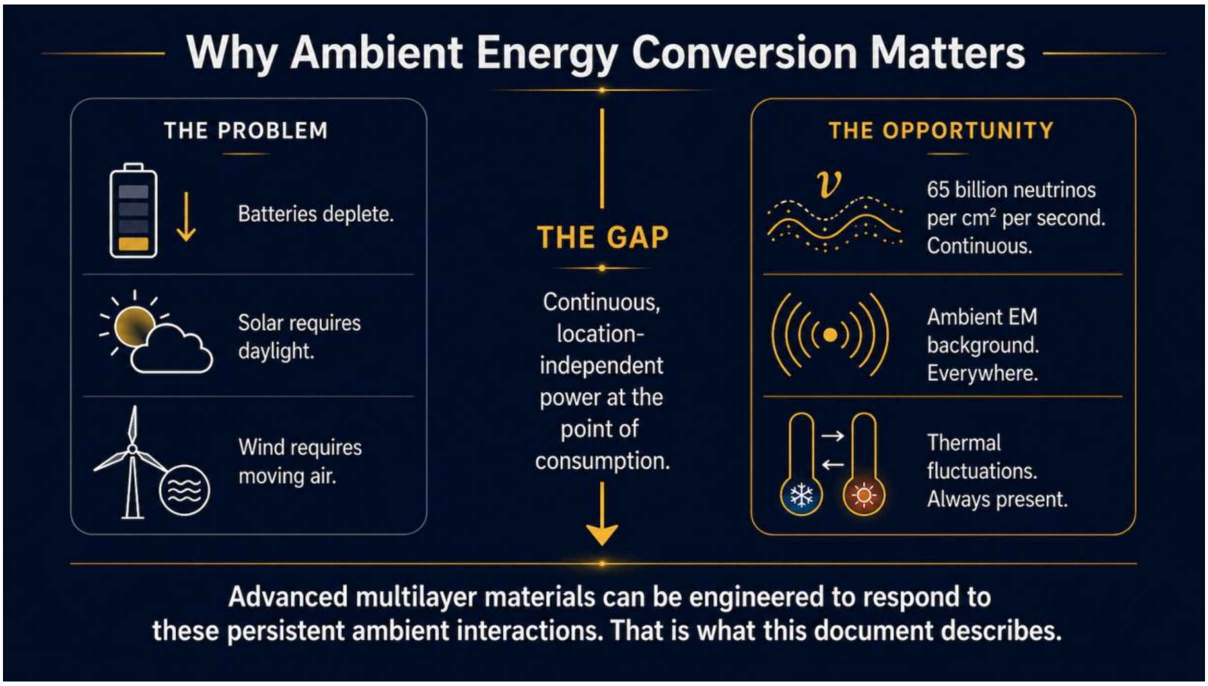

1. Historical Milestones

The physics behind this framework was established independently, by institutions with no connection to the Neutrino Energy Group, over nearly four decades.

- **1987, Supernova 1987A:** the first neutrinos detected from an astrophysical source beyond the Sun, recorded by Kamiokande II and IMB. Phys. Rev. Lett. 58, 1490. This was the first direct evidence that neutrino flux from beyond the solar system is real and arrives continuously.
- **2015, Nobel Prize in Physics:** awarded to Kajita and McDonald for the discovery of neutrino oscillations, proving neutrinos carry mass. Mass means momentum, and momentum means neutrino-matter interaction involves a real physical transfer, not a particle passing through matter without consequence.
- **2017, CEvNS confirmed:** the COHERENT collaboration reported the first observation of coherent elastic neutrino-nucleus scattering. Akimov et al., Science 357, 1123–1126. This is the coupling mechanism the framework below depends on directly.
- **2025, JUNO Observatory:** precision neutrino flux measurements begin, continuing to refine the physical parameters this model integrates.

Each milestone was achieved independently, and each confirms a physical assumption the framework already depends on.

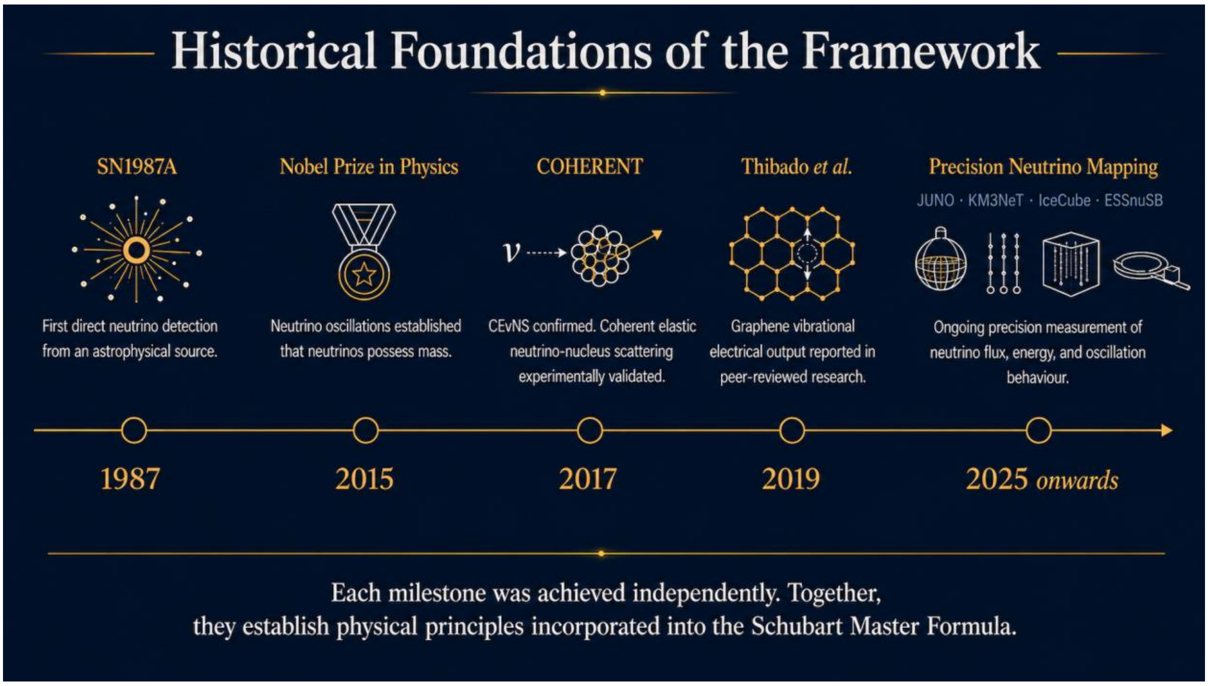

2. What Makes This Different

Photovoltaic systems need sunlight and stop generating when it is gone. Neutrinovoltaic systems convert ambient interactions that are present regardless of daylight, cloud cover, or time of day.

Wind turbines need moving air at sufficient velocity, and cannot be deployed at most points of consumption. Neutrinovoltaic systems have no moving parts and no atmospheric precondition.

Batteries store energy generated somewhere else, then deplete and need recharging. Neutrinovoltaic systems generate continuously, at the point of consumption, from sources that are never absent.

Nuclear reactors generate continuous baseload power but require fuel, cooling infrastructure, and centralised deployment. Neutrinovoltaic systems are distributed, solid-state units that require none of that.

The distinguishing characteristic is not what the system produces. It is what it does not require.

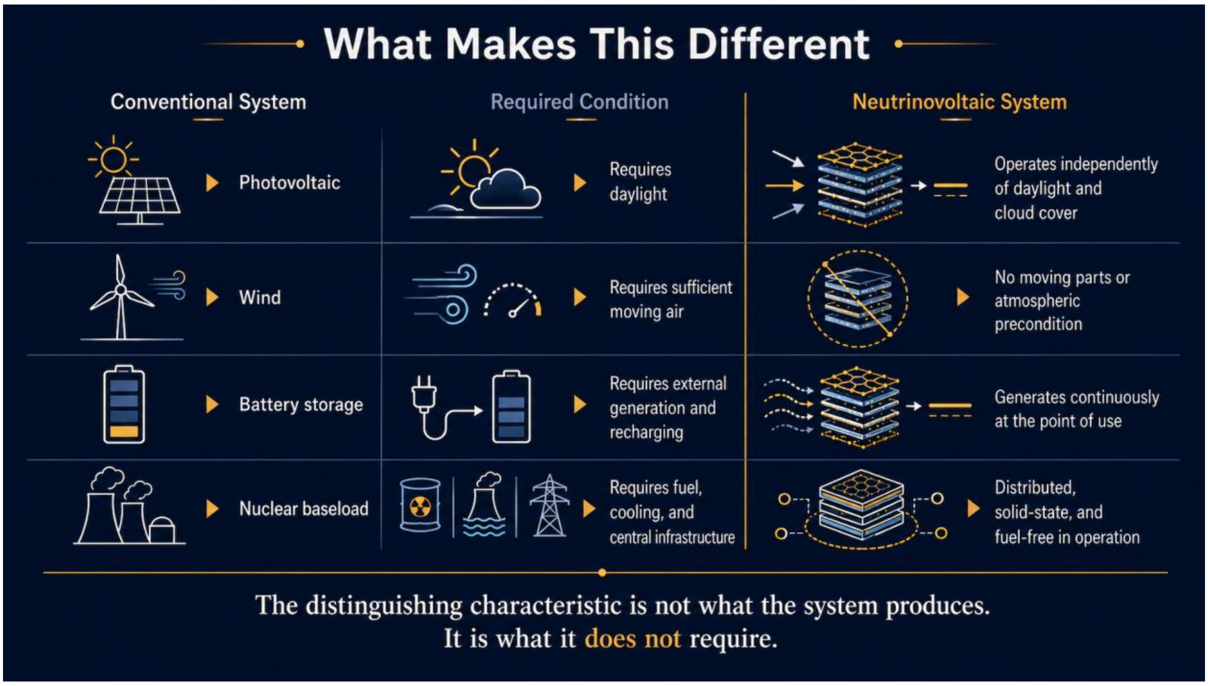

3. Core Physical Mechanism: CEvNS

Coherent Elastic Neutrino-Nucleus Scattering (CEvNS) is the foundational interaction in neutrinovoltaic technology. Instead of scattering off an individual proton or neutron, a neutrino scatters coherently off an entire nucleus, producing a nuclear recoil that transfers momentum directly into the material lattice.

Cross-section: $\sigma \propto N^2 \cdot E_\nu^2$

where N is the neutron number of the target nucleus and E_ν is the neutrino energy. Because the interaction is coherent, the cross-section scales with the square of the neutron number rather than linearly with nucleon count, producing an effective interaction probability orders of magnitude larger than single-nucleon estimates would suggest. This is what makes an otherwise vanishingly weak interaction usable at all.

Two further effects amplify the coupling beyond the baseline CEvNS cross-section. Non-Standard Interactions (NSI) are theoretically motivated extensions to the coupling that modify its effective strength under specific material and field conditions. Oblique scattering geometries, recoil events that are not purely forward-directed, increase the population of interactions that transfer usable momentum into the lattice rather than passing through it unfelt.

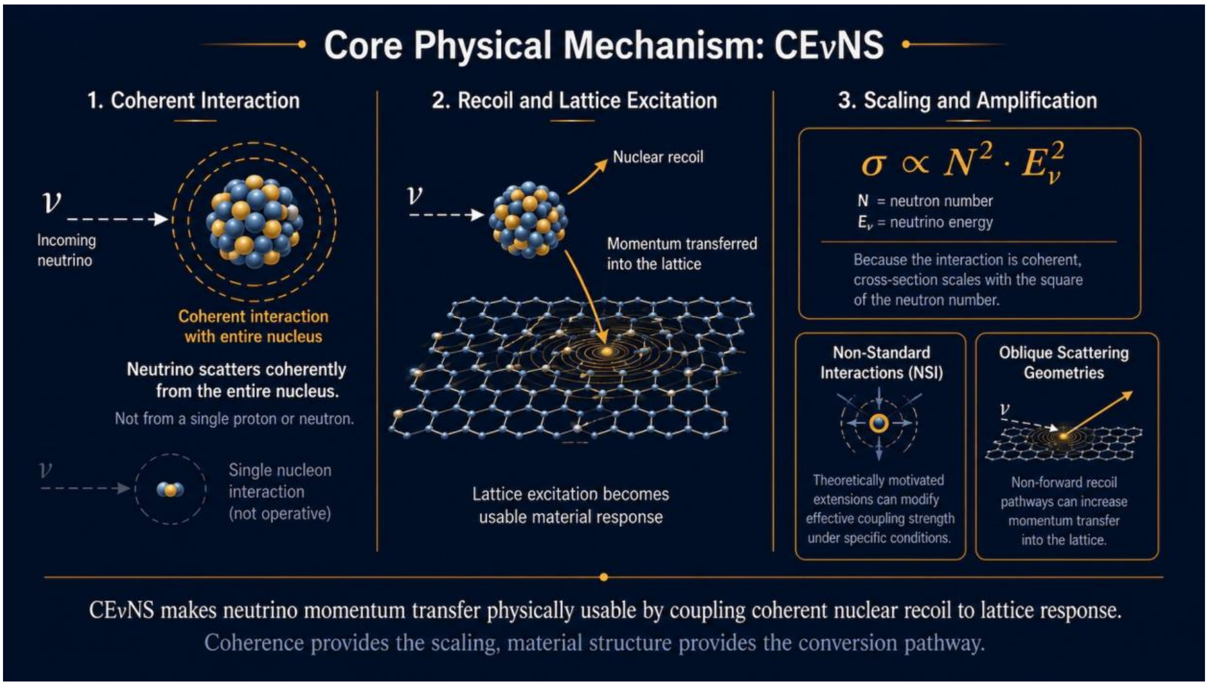

4. The Material System

Section 3 establishes that momentum arrives continuously. This section is about the structure engineered to catch it.

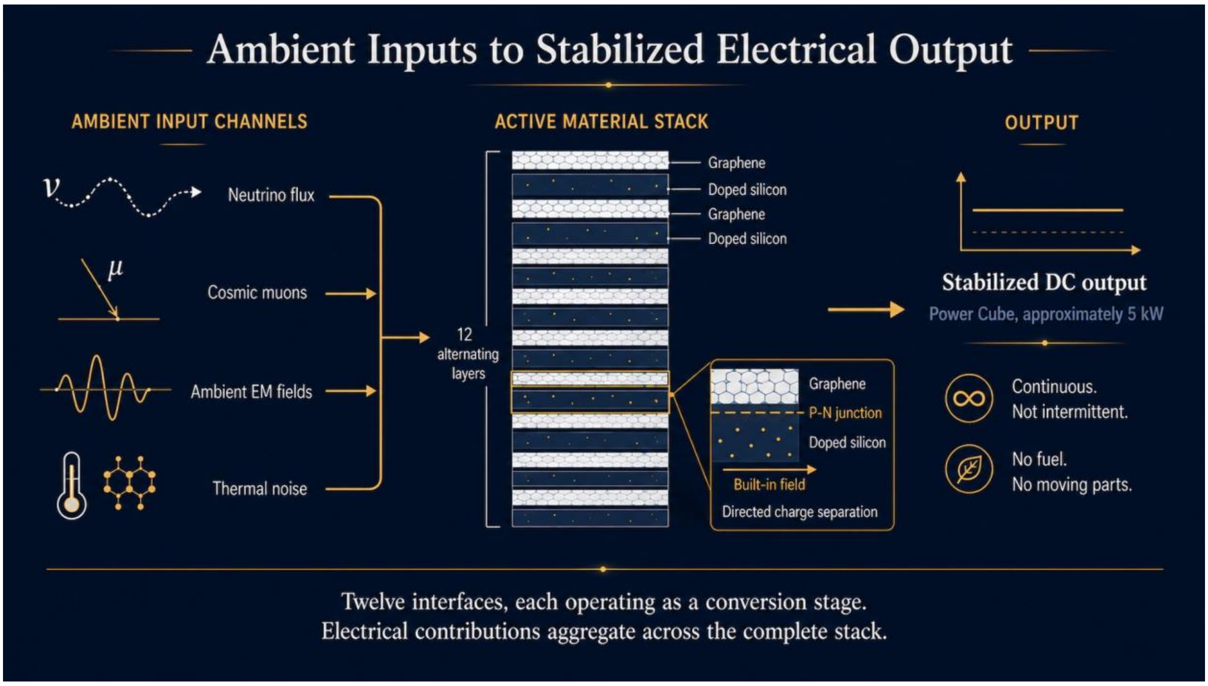

Graphene

Graphene has the highest charge carrier mobility of any known material, which is what allows a momentum disturbance at one point in the lattice to become an electronic signal rather than dissipating as heat before it can be used. Two properties make it specifically suited to this role.

First, direct phonon-electron coupling: mechanical lattice vibration transfers energy straight into the electronic system rather than through an intermediate thermal step, which is the difference between a usable signal and waste heat. Second, plasmon resonance: graphene supports collective electron oscillations that resonantly amplify its response to ambient electromagnetic fields, which is the physical basis of the EM channel in the Master Formula below.

Mechanically, a graphene layer behaves like a nanoelectromechanical (NEMS) resonator, oscillating with quality factors (Q) up to 10^4. A high Q-factor means the layer loses very little vibrational energy to internal damping per oscillation cycle, so momentum arriving from any input channel stays available to the electronic system for many cycles rather than being lost immediately. This is the material property that makes a weak, continuous input usable at all: the layer holds onto the energy long enough to convert it.

Doped Silicon

Doped silicon layers sit at each graphene interface. P-N junctions at these interfaces create a built-in electric field, which is what turns a symmetric, non-directional vibration into a directed drift current: without that built-in asymmetry, electrons driven by the vibration would simply move back and forth with no net current. The same interfaces also produce resonance amplification, reinforcing the mechanical response of the adjacent graphene layer rather than damping it.

Architecture

The stack is twelve alternating layers of graphene and doped silicon. Each interface is a separate conversion stage: the graphene layer responds mechanically and electronically to the four input channels, the adjacent silicon junction rectifies that response into directed current, and the next layer down does the same, independently.

Because the stack is many layers deep rather than a single surface, penetrating flux, neutrinos and muons in particular, interacts with every layer on its way through rather than stopping at the first one. Output scales with active material volume, not with the surface area presented to any single incoming flux, which is the direct engineering answer to the standard objection that individual interaction cross-sections are too small to matter in practice: twelve interfaces, each contributing independently, multiply what one interface cannot produce alone.

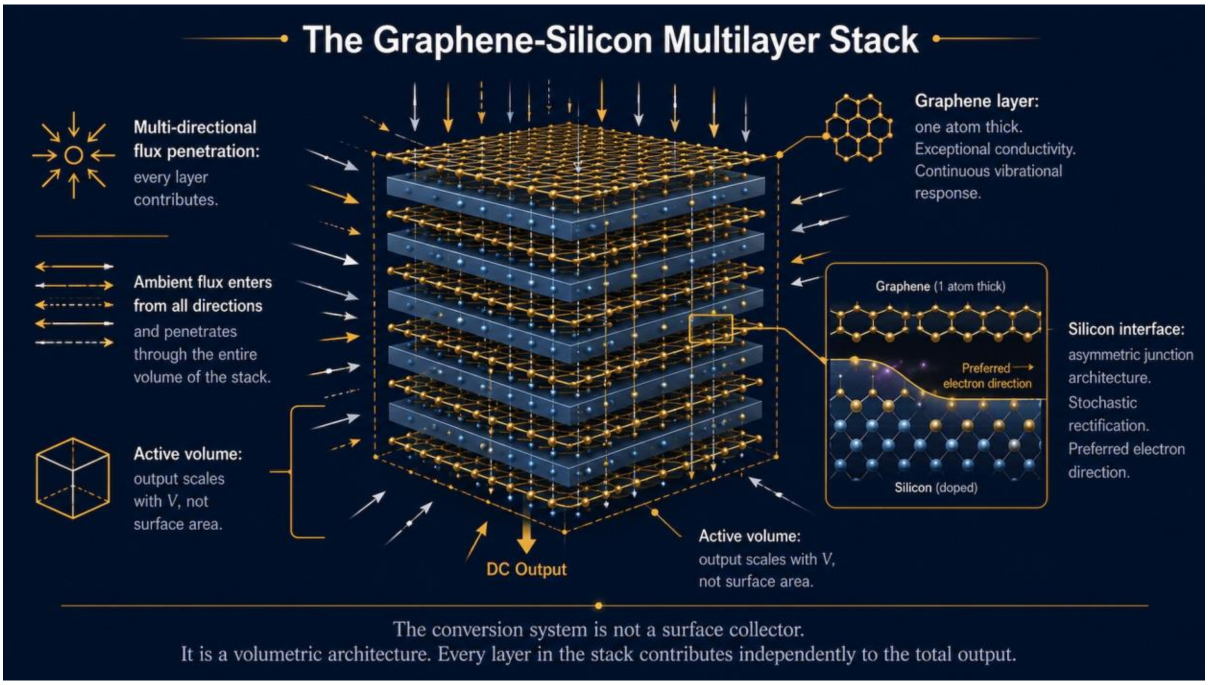

5. The Six-Stage Conversion Chain

Stage 1, Momentum Transfer. Four input channels feed the stack simultaneously: CEvNS nuclear recoils in the electronvolt-to-kiloelectronvolt range, cosmic muon energy deposition, electromagnetic coupling via plasmon resonance, and thermal fluctuations providing a continuous baseline.

Stage 2, Mechanical Response. The graphene layer vibrates resonantly in response. Oscillation amplitude scales as $Q \cdot F/m\omega^2$, where Q is the quality factor described above, F is the driving force from the input channels, m is the effective mass of the resonating layer, and ω is the driving frequency.

Stage 3, Phonon-Electron Coupling. Lattice deformation shifts the position of graphene's Dirac points, the points in its electronic band structure where conduction and valence bands meet. The shift is $\Delta E_D \approx D \cdot \nabla \cdot u$, where D is the deformation potential and $\nabla \cdot u$ is the local strain. This shift generates an alternating voltage, $V_{ac}(t)$, across the layer.

Stage 4, Nonlinear Rectification. Schottky contacts and P-N junctions at the silicon interfaces rectify the alternating signal into direct current: $I_{DC} \approx \frac{1}{4} \cdot (d^2I/dV^2) \cdot V_{rms}^2$, a standard nonlinear rectification relationship applied here across every junction in the stack.

Stage 5, Layer Summation. Currents generated at all twelve interfaces add constructively, multiplying total output rather than merely averaging it.

Stage 6, DC Stabilization. Power-management integrated circuits smooth and stabilize the summed output into clean, continuous direct current suitable for end-use applications.

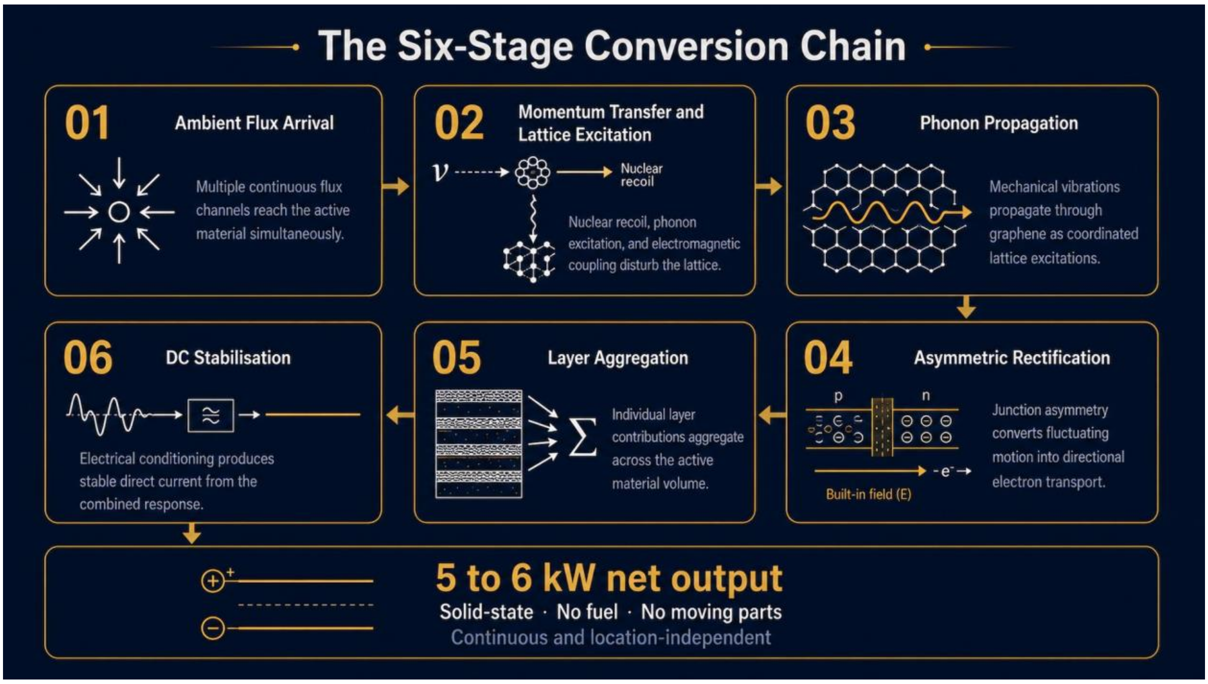

6. The Master Formula

$$I_{NV} = \alpha \int \Phi_{\nu}(E) \cdot \sigma_{CE\nu NS}(E) \cdot \Delta p(E)\, dE + \beta \cdot \Phi_{\mu} \cdot \langle \Delta E_{\mu} \rangle + \gamma \cdot \Phi_{EM} \cdot \eta_{plasmon} + \delta \cdot \Phi_{th} \cdot k_B \cdot T$$

Four additive terms represent the complete energy input spectrum, each corresponding to one of the four channels in Stage 1 above.

- **Neutrino term (α):** the integral over the neutrino energy spectrum of flux $\Phi_{\nu}(E)$, the CEvNS cross-section $\sigma_{CE\nu NS}(E)$ from Section 3, and the momentum transfer $\Delta p(E)$ at each energy. This is the primary mechanism.
- **Muon term (β):** the ambient cosmic muon flux Φ_{μ}, roughly 100 muons per square metre per second at sea level, multiplied by the average energy deposited per muon, $\langle \Delta E_{\mu} \rangle$.

- **Electromagnetic term (γ):** ambient electromagnetic radiation Φ_EM coupled through plasmon resonance efficiency η_plasmon, the same graphene property described in Section 4.
- **Thermal term (δ):** ambient thermal flux Φ_th harvested via stochastic resonance, scaled by k_B · T, the Boltzmann constant times absolute temperature, the standard thermal energy scale.

No single term is required to dominate. The architecture is built for all four channels to contribute simultaneously, which is why output remains continuous even as any one channel's contribution fluctuates with location, altitude, or ambient conditions.

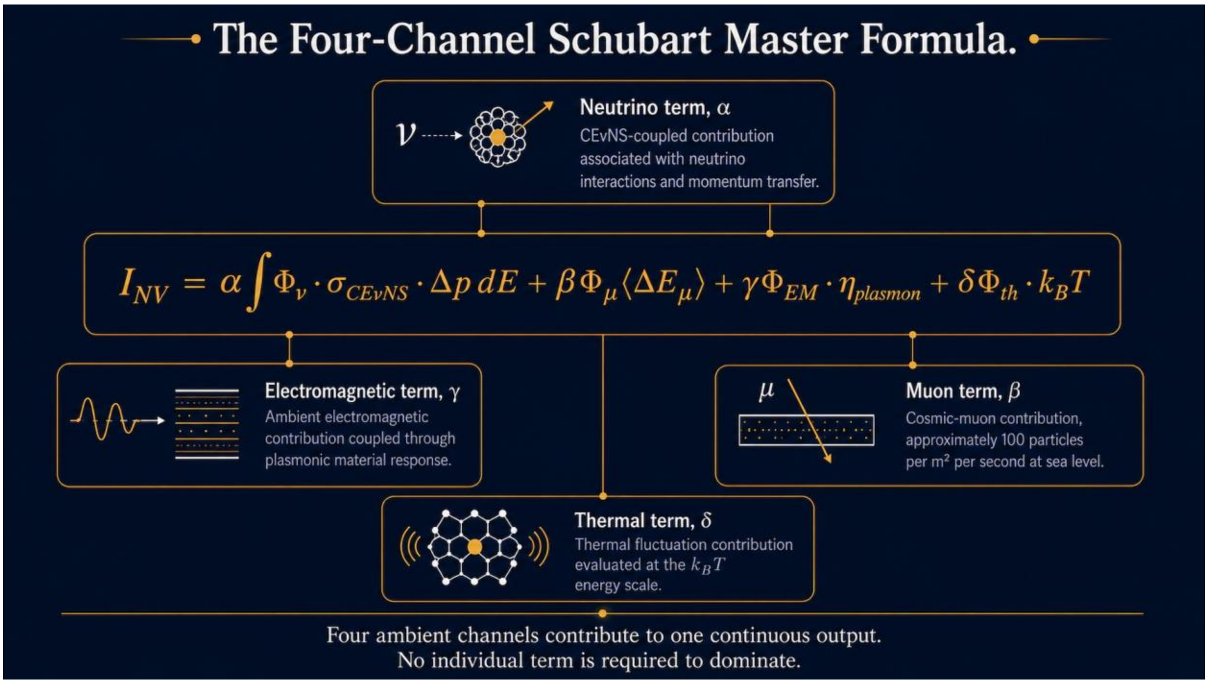

7. Performance Parameters

Parameter	Value
Theoretical output	3–5 kW per 1,500 m² active surface
Power Cube output	≈5 kW continuous (24/7)
Temperature variation, unregulated	±15%
Temperature variation, regulated	±3–5%
Operation	Weather-independent, day and night

8. Applications

- **Power Cube:** a standalone unit delivering approximately 5 kW of continuous power for residential and commercial use, with no fuel and no grid connection required.
- **Pi Car:** vehicle integration providing continuous auxiliary power or primary propulsion assist, drawing on the same multilayer architecture described in Section 4.
- **Pi-12 Platform:** a scalable, modular platform for industrial applications, built around the same twelve-layer conversion stack at larger scale.
- **Sensor Systems:** low-power autonomous sensors for remote and IoT deployments, where the absence of a battery-replacement cycle is often the deciding factor.

9. Core Patent

WO2016142056A1 (2016): "Method for energy generation from radiation using graphene-silicon multilayers."

10. Key References

1. Hirata, K. et al. / Kamiokande II Collaboration (1987). Observation of a neutrino burst from Supernova SN1987A. Physical Review Letters 58, 1490-1493.
2. Fukuda, Y. et al. / Super-Kamiokande Collaboration (1998). Evidence for oscillation of atmospheric neutrinos. Physical Review Letters 81, 1562-1567.
3. Ahmad, Q.R. et al. / SNO Collaboration (2002). Direct evidence for neutrino flavour transformation from neutral-current interactions in the Sudbury Neutrino Observatory. Physical Review Letters 89, 011301.
4. Eguchi, K. et al. / KamLAND Collaboration (2003). First results from KamLAND: Evidence for reactor antineutrino disappearance. Physical Review Letters 90, 021802.
5. The Nobel Committee for Physics (2015). Nobel Prize in Physics 2015: Discovery of neutrino oscillations, showing that neutrinos have mass.
6. Particle Data Group (2024). Review of Particle Physics. Progress of Theoretical and Experimental Physics. Latest edition.
7. Freedman, D.Z. (1974). Coherent effects of a weak neutral current. Physical Review D 9, 1389-1392.
8. Drukier, A. & Stodolsky, L. (1984). Principles and applications of a neutral-current detector for neutrino physics and astronomy. Physical Review D 30, 2295-2309.
9. Akimov, D. et al. / COHERENT Collaboration (2017). Observation of coherent elastic neutrino-nucleus scattering. Science 357, 1123-1126.
10. Akimov, D. et al. / COHERENT Collaboration (2021). First detection of coherent elastic neutrino-nucleus scattering on argon. Physical Review Letters 126, 012002.
11. Barranco, J., Miranda, O.G. & Rashba, T.I. (2005). Probing new physics with coherent neutrino scattering off nuclei. Physical Review D 72, 113009.
12. An, F. et al. / JUNO Collaboration (2016). Neutrino physics with JUNO. Journal of Physics G 43, 030401.
13. Aartsen, M.G. et al. / IceCube Collaboration (2013). Evidence for high-energy extraterrestrial neutrinos at the IceCube detector. Science 342, 1242856.
14. Abi, B. et al. / DUNE Collaboration (2020). Long-baseline neutrino oscillation physics potential of the DUNE experiment. European Physical Journal C 80, 978.
15. Novoselov, K.S. et al. (2004). Electric field effect in atomically thin carbon films. Science 306, 666-669.
16. Castro Neto, A.H. et al. (2009). The electronic properties of graphene. Reviews of Modern Physics 81, 109-162.
17. Geim, A.K. & Novoselov, K.S. (2007). The rise of graphene. Nature Materials 6, 183-191.
18. Bolotin, K.I. et al. (2008). Ultrahigh electron mobility in suspended graphene. Solid State Communications 146, 351-355.

19. Ferrari, A.C. et al. (2006). Raman spectrum of graphene and graphene layers. Physical Review Letters 97, 187401.
20. Piscanec, S. et al. (2004). Kohn anomalies and electron-phonon interactions in graphite. Physical Review Letters 93, 185503.
21. Bunch, J.S. et al. (2007). Electromechanical resonators from graphene sheets. Science 315, 490-493.
22. Grigorenko, A.N., Polini, M. & Novoselov, K.S. (2012). Graphene plasmonics. Nature Photonics 6, 749-758.
23. Jablan, M., Buljan, H. & Soljačić, M. (2009). Plasmonics in graphene at infrared frequencies. Physical Review B 80, 245435.
24. Koppens, F.H.L. et al. (2011). Graphene plasmonics: A platform for strong light-matter interactions. Nano Letters 11, 3370-3377.
25. Thibado, P.M. et al. (2020). Fluctuation-induced current from freestanding graphene. Physical Review E 102, 042101.
26. Crossno, J. et al. (2016). Observation of the Dirac fluid and the breakdown of the Wiedemann-Franz law in graphene. Science 351, 1058-1061.
27. Prigogine, I. (1977). Nobel Lecture: Time, structure and fluctuations.
28. Prigogine, I. & Nicolis, G. (1977). Self-Organization in Non-Equilibrium Systems. Wiley.
29. Gammaitoni, L. et al. (1998). Stochastic resonance. Reviews of Modern Physics 70, 223-287.
30. Geim, A.K. & Grigorieva, I.V. (2013). Van der Waals heterostructures. Nature 499, 419-425.
31. Novoselov, K.S. et al. (2016). 2D materials and van der Waals heterostructures. Science 353, aac9439.
32. Liu, Y. et al. (2016). Van der Waals heterostructures and devices. Nature Reviews Materials 1, 16042.
33. CODATA (2022). CODATA recommended values of the fundamental physical constants. Reviews of Modern Physics.
34. Schubart, H.T. et al. (2016). Method for Energy Generation from Radiation Using Graphene-Silicon Multilayers. International Patent WO2016142056A1. Foundational engineering framework for multilayer neutrinovoltaic energy conversion.

Disclaimer

This document presents the theoretical framework and research status of neutrinovoltaic technology. Quantitative predictions require independent experimental validation. The physics allows the described mechanisms; measurement decides. This is not investment advice.

Prepared by an interdisciplinary working group of scientists, engineers, and technical contributors active in the fields of particle physics, condensed matter physics, nanomaterials science, graphene research, non-equilibrium thermodynamics, and applied mathematics.

This document is based on internationally published experimental results, peer-reviewed scientific literature, established findings of modern physics, and mathematical consistency analyses conducted in connection with the Schubart Master Formula and neutrinovoltaic energy conversion architectures.

Coordinated within the Scientific Advisory Board of the Neutrino® Energy Group.

On behalf of the Board

Geneva, Switzerland — July 2026